Journal of
Nanoelectronics and Optoelectronics
Vol. 17, pp. 758–768, 2022
www.aspbs.com/jno

ARTICLE

Study on Noise Reduction of Tunable Diode Laser Absorption Spectroscopy Detection Signal Based on Complete Ensemble Empirical Mode Decomposition with Adaptive Noise-Detrended Fluctuation Analysis-Wavelet Soft Threshold

An-Sheng Zhao[1], Xu Yang[1,*], Xiao-Feng An[2], He Zhang[3], and Shi-Da Zhang[4]

Tunable diode laser absorption spectroscopy (TDLAS) is a significant technique for measuring gas concentration in the combustion field. When the gas concentration is detected by wavelength modulation spectroscopy, the second harmonic (2f) signal demodulated by a lock-in amplifier can be analyzed to obtain the gas concentration information. However, the 2f signal will be affected by the white Gaussian noise of electronic equipment and the optical fringe of the standard instrument, which will lead to the reduction of the gas detection accuracy. To solve the above problems, this paper proposes a 2f signal noise reduction algorithm based on the complete ensemble empirical mode decomposition with adaptive noise (CEEMDAN), detrended fluctuation analysis (DFA), and wavelet soft threshold (WST). Taking CO_2 gas as an example, the 2f signal extracted from the experiment was denoised, and the amplitude of the 2f signal was linearly fitted to the gas concentration. The R^2 value was 0.9979, and the SNR was 31.9750 dB. The denoising effect is obvious, and the denoising algorithm can better retain the peak information of the second harmonic signal. In this paper, the existing classical noise reduction algorithm is simulated and analyzed. To display the noise reduction effect visually in the time-frequency domain, the Hilbert-Huang transform three-dimensional spectrum is introduced to analyze the spectrum characteristics of the noise reduction signal.

Keywords: Tunable Diode Laser Absorption Spectroscopy, Second Harmonic, Complete Ensemble Empirical Mode Decomposition With Adaptive Noise (CEEMDAN), Detrended Fluctuation Analysis (DFA), Wavelet Soft Threshold (WST), Hilbert-Huang Transform (HHT).

1. INTRODUCTION

Tunable diode laser absorption spectroscopy (TDLAS) has the characteristics of high sensitivity and strong stability [1]. It is often used in atmospheric monitoring, combustion field diagnosis, and human respiration detection [2]. TDLAS gas detection technology includes direct absorption spectroscopy technology and wavelength modulation technology. Wavelength modulation spectroscopy technology has higher sensitivity than direct absorption spectroscopy technology [3]. When wavelength modulation spectroscopy technology is applied to open gas detection, it will be affected by some uncontrollable environmental noise, noise in optical components and electronic devices, and optical fringes, resulting in the second harmonic (2f) signal is not smooth enough, the peak information is not clear, and the accuracy of concentration measurement will be affected [4].

[1]School of Electronic Information Engineering, Changchun University of Science and Technology, Changchun 130022, China
[2]Jilin Engineering Normal University, ChangChun 130103, China
[3]State Key Laboratory of High Power Semiconductor Lasers, Changchun University of Science and Technology, Changchun 130022, China
[4]State Key Laboratory of Applied Optics, Changchun Institute of Optics, Fine Mechanics and Physics, Chinese Academy of Sciences, Changchun 130033, China
*Author to whom correspondence should be addressed.
Email: lbaomi@cust.edu.cn
Received: 11 February 2022
Accepted: 17 April 2022

 1555-130X/2022/17/758/011 doi:10.1166/jno.2022.3248

At present, the research on improving the accuracy of gas detection mainly includes hardware design and software denoising. In terms of hardware design, Zhu et al. proposed a light source that can continuously modulate the wavelength and achieve a constant output power, which can suppress the spectral distortion of 2f signal and improve the accuracy of gas detection [5]. Yang et al. used two-tone modulation combined with vibrational reflectors to solve the problem of background fluctuations caused by light interference fringes in TDLAS systems [6]. Kireev et al. improved the detection accuracy of the system by using synchronous detection technology of tunable diode lasers modulated by pumped current frequency, combined with the application of the Wiener filtering algorithm [7]. Chong et al. designed the BRD circuit to suppress the residual amplitude modulation caused by the second harmonic signal distortion and improve the accuracy of measurement [8]. These methods can improve the detection accuracy of the system but will increase the complexity of the TDLAS system. In terms of software denoising, Bin et al. used Gabor transform to de-noise the 2f signal, which improved the SNR of the system by 15.73 dB [9]. Wang et al. applied singular value decomposition to noise reduction of second harmonic signals, achieving a system noise removal rate of 80% [10]. Liu and YS used wavelet transform to perform baseline elimination and noise filtering for the second harmonic signal, and the relative error between the processed signal and the theoretical signal decreased from 1.26% to 0.12% [11]. Li et al. used wavelet transform to effectively suppress interference signals [12]. Cai et al. introduced an equal-weight sampling strategy, which reduced noise by 11% [13]. Lu et al. proposed an adaptive progressive Savitzky-Golay (S-G) smoothing filtering algorithm to filter the spectral signal and remove the noise better [14]. Zheng et al. used an improved LMS adaptive denoising algorithm to effectively suppress the interference of strong noise in the spectrum [15]. Liang et al. used a variational mode decomposition filtering algorithm to denoise the 2f signal, and the denoised 2f amplitude was fitted to the gas concentration, and the R^2 increased from 0.9633 to 0.9940 [16]. With the deepening of research, aiming at the shortcomings of the single filter algorithm, some joint noise reduction algorithms have been proposed, such as the Empirical Mode Decomposition (EMD) and wavelet threshold (WT) denoising algorithm [17], complete ensemble empirical mode decomposition with adaptive noise (CEEMDAN) and WT combined denoising algorithm [18]. The key technology of these joint denoising algorithms is to solve the discriminant problem of noise intrinsic mode functions (IMFs) obtained by CEEMDAN decomposition. The commonly used discriminant method is the mean square error criterion, but if there are continuous IMFs components whose MEAN square error value is close, it is difficult to discriminate the noise signal.

Based on the existing research, a CEEMDAN, detrended fluctuation analysis (DFA), and wavelet soft threshold (WST) are proposed. Further, suppress the noise in the 2f signal and extract the useful 2f signal. This method uses the DFA algorithm to solve the problem of IMFs component discrimination of noise. The second harmonic signal with noise is decomposed by CEEMDAN, and the information-dominated IMFs component is screened by the DFA algorithm. The information-dominated IMFs component is reconstructed, and the reconstructed signal is further de-noised by using the WST to obtain the de-noised second harmonic signal. The proposed algorithm is compared with CEEMDAN-DFA-Wavelet Hard Threshold (WHT), CEEMDAN-WST, CEEMDAN-WHT, EMD-DFA-WST, WST, and WHT methods for simulation and analysis of noise reduction effects. The results show that the denoising method has a better suppression effect on 2f signal noise.

2. CEEMDAN-DFA-WST DENOISING PRINCIPLE

2.1. CEEMDAN-DFA-WST Denoising Algorithm Flow

The CEEMDAN-DFA-WST denoising steps of TDLAS proposed in this paper are:

Step 1: CEEMDAN decomposes noisy signals into various order IMFs.

Step 2: The Hurst index values of IMF components were calculated by the DFA method.

Step 3: Remove the IMF components whose Hurst index is less than 0.5 and reconstruct the remaining IMF components to obtain the reconstruction signal.

Step 4: The reconstructed signal is denoised by wavelet soft threshold and the denoised second harmonic signal is obtained.

CEEMDAN-DFA-WST denoising process is shown in Figure 1.

2.2. Principle of the CEEMDAN

CEEMDAN is an improved algorithm based on EMD and ensemble empirical mode decomposition (EEMD). EMD can decompose any signal into the form of IMFs with different frequencies and can process non-stationary nonlinear signals adaptively, but its decomposition has modal aliasing [19]. EEMD can solve this problem, but the decomposition method has the problem of noise residue. Complementary ensemble Empirical Mode decomposition (CEEMD) can suppress the noise residue problem, but its improper parameter selection may lead to the existence of false IMFs [20]. Based on CEEMD, TORRES proposed the CEEMDAN decomposition algorithm [21], which can obtain pure IMFs and perform signal decomposition adaptively [22], providing a distinct advantage in processing nonlinear and non-stationary signals. CEEMDAN decomposition steps are as follows:

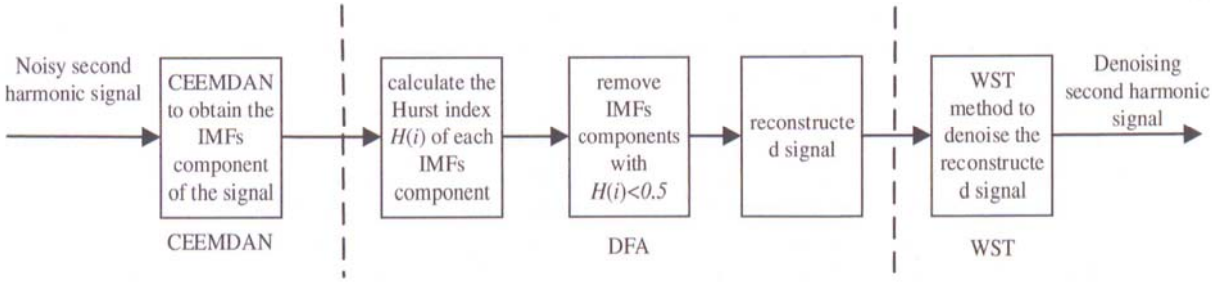

Fig. 1. Flow chart of CEEMDAN-DFA-WST denoising method.

Step 1: Add white noise to the signal to be processed $X(t)$, and obtain N IMFs after EMD decomposition. Set to $a_1, a_2, \ldots a_N$, the components of the first-order eigen mode function after CEEMDAN decomposition are obtained:

$$\overline{a_1(t)} = \frac{1}{N}\sum_{j=1}^{N} a_1^j(t), j = 1, 2 \ldots N \tag{1}$$

Step 2: When $j = 1$, calculate the residual error:

$$r_1(t) = x(t) - \overline{a_1(t)} \tag{2}$$

Step 3: Add the positive and negative white noise signals into $r_1(t)$ to obtain signal $y(t)$. After the decomposition of EMD with $y(t)$, the first-order eigen mode component b_1 can be obtained, then:

$$\overline{a_2(t)} = \frac{1}{N}\sum_{j=1}^{N} b_1^j(t), j = 1, 2, \ldots N \tag{3}$$

Step 4: Calculate residual:

$$r_2(t) = r_1(t) - \overline{a_2(t)} \tag{4}$$

Step 5: Repeat the above steps until $r(t)$ is indecomposable. At this time, k IMF are obtained, then the signal to be processed can be expressed as:

$$x(t) = \sum_{k=1}^{K} \overline{a_k(t)} + r_k(t) \tag{5}$$

2.3. Principle of the DFA

In the improved denoising algorithm of CEEMDAN, the distinction between the information-dominated IMF component and the noise-dominated IMF component is the key to the denoising effect. The artificial discrimination method lacks self-adaptability and is easy to cause large errors. DFA algorithm is introduced, which can provide a quantitative parameter, namely Hurst index, Hurst exponent can reflect the long-range power-law correlation of non-stationary signals [23], therefore, the IMFs component of noise can be accurately determined. The steps of DFA algorithm are as follows:

Step 1: As shown in Eq. (6), non-stationary time series $x(t)$ is processed to obtain signal $x'(k)$:

$$x'(k) = \sum_{i=1}^{k} (x(t) - \bar{x}), k = 1, 2 \ldots, N \tag{6}$$

Where, N is the length of time series $x(t)$, and $\bar{x}$ is the mean value of $x(t)$.

Step 2: Divide $x'(k)$ into n non-overlapping sub-sequences and fit the sub-sequences. Suppose that the local linear trend of these sub-sequence segments is $y_n(k)$, then the root mean square fluctuation is:

$$F_n = \sqrt{\frac{1}{N}\sum_{k=1}^{N} (x'(k) - y_n(k))^2} \tag{7}$$

Step 3: If $x(t)$ has long range power law correlation, then

$$F_n \infty n^{\alpha} \tag{8}$$

Where, α is the scale index.

α is used to represent the long-range power law correlation of the sequence. When $\alpha < 0.5$, the sequence is considered to have anti-persistence; when $\alpha = 0.5$, the sequence is considered to be random; when $\alpha > 0.5$, the sequence is considered to be continuous [24]. In signal denoising, it can be considered that when $\alpha < 0.5$, the signal has short-range correlation and noise is considered as the dominant component. Therefore, whether the IMF component is the dominant component of noise can be determined by calculating the value of α.

2.4. Wavelet Threshold Denoising

The wavelet transform has a good ability to express local features in the time-frequency domain and has good applicability to the analysis of non-stationary signals and local features. It can denoise signals by selecting appropriate thresholds [25]. The commonly used threshold denoising methods include wavelet hard threshold (WHT) denoising and wavelet soft threshold (WST) denoising [26]. WHT is better than WST in the mean square sense, but there are jump points in the denoised signal, and the signal is not smooth enough, which affects the extraction accuracy of the peak point information of the second harmonic signal. Although the wavelet soft threshold has the advantages of a smooth denoising effect and good continuity, it will compress the signal, lead to certain deviations and affect the accuracy of signal reconstruction. The WST method is adopted in this paper.

WHT denoising method:

$$\varpi_\lambda = \begin{cases} \varpi & |\varpi| \geq \lambda \\ 0 & |\varpi| < \lambda \end{cases} \tag{9}$$

Where, ϖ_λ is the wavelet coefficient, ϖ is the wavelet decomposition coefficient, and λ is the critical threshold. Set it to 0 when $|\varpi| > \lambda$ and leave it the same when $|\varpi| \geq \lambda$.

Wavelet soft threshold denoising method:

$$\varpi_\lambda = \begin{cases} [\mathrm{sgn}(\varpi)](|\varpi| - \lambda) & |\varpi| \geq \lambda \\ 0 & |\varpi| < \lambda \end{cases} \tag{10}$$

Where, ϖ_λ is the wavelet coefficient, $\mathrm{sgn}(\cdot)$ is the sign function, ϖ is the wavelet decomposition coefficient, and λ is the critical threshold. When $|\varpi| < \lambda$, set it to 0; when $|\varpi| \geq \lambda$, set it to the difference between the point value and the threshold value.

3. SIMULATION AND ANALYSIS

3.1. Measuring Principle

The Beer-Lambert law, which describes the relationship between spectral line parameters and environmental conditions and the absorption rate of light, is the theoretical cornerstone of the TDLAS technology. The law applies to all molecules and atoms whose states can absorb photons.

According to the Beer-Lambert law, the absorption coefficient of light is proportional to the product of optical path and concentration. When an incident light with intensity I_0 is absorbed through a gas with length L, the transmitted light intensity I_t can be expressed as:

$$I_t = I_0 \exp[-PS(T)g(v)CL] \tag{11}$$

Where, P is the total pressure (unit: atm), I_t is the transmitted light intensity, I_0 is the incident light intensity, $S(T)$ is the line intensity, $g(v)$ is the linear function of the spectral line, C is the gas concentration, and L is the absorption optical path length.

In the low-concentration CO_2 detection experiment, the absorbed signal detected by the detector is very weak. In wavelength modulation technology, a lock-in amplifier is used to modulate and demodulate the input original harmonic signal to generate the 2f Signal. Since the signal is modulated and demodulated, it will be removed in the subsequent signal processing compared with the direct absorption technique, thus reducing the influence of external background signals.

The second harmonic component after demodulation is:

$$H_2(x,m) = -\frac{2PS(T)CL}{\pi\Delta v_c} \times \left[\frac{4}{m^2} - \frac{\sqrt{2}(M+1-x^2)\sqrt{\sqrt{M^2+4x^2}+M}}{m^2\sqrt{M^2+4x^2}} - \frac{4x\sqrt{\sqrt{M^2+4x^2}-M}}{m^2\sqrt{M^2+4x^2}}\right] \tag{12}$$

Where H_2 is the cosine Fourier coefficient of the laser transmittance, m is the modulation depth, $M = 1 - x^2 + m^2$, Δv_c is the collision linewidth, and when $x = 0$, the amplitude of the 2f signal at the center frequency is:

$$H_2(0,m) = -\frac{2PS(T)CL}{\pi\Delta v_c}\left[\frac{4}{m^2} - \frac{2(2+m^2)}{m^2\sqrt{1+m^2}}\right] \tag{13}$$

As can be seen from the above equation, after the modulation depth m is determined, the 2f signal related to the gas concentration is obtained.

3.2. Simulation Experiments

In the TDLAS system, the 2f signal. Will be affected by the white Gaussian noise of electronic devices and the optical interference fringe effect. Taking the absorption spectral line of carbon dioxide gas at 1572.3 nm as an example, the effectiveness of the CEEMDAN-DFA-WST noise reduction algorithm was verified. Simulink simulation platform was used to simulate the TDLAS gas detection system, and the ideal second-harmonic signal extracted by lock-in amplifier in wavelength modulation technology was simulated, as shown in Figure 2(a). The wavelength of the interference fringe is generally in the order of $10^{-3}\sim10^{-2}$ cm^{-1}, which is directly superimposed on the harmonic signal in the form of the sine wave. The second harmonic signal superimposed on the interference fringe is shown in Figure 2(b). In the actual experiment, white Gaussian noise and optical interference fringe will affect the detection accuracy of the system simultaneously. In this paper, the random number module is used to add Gaussian white noise signal to the ideal signal, and the optical interference fringe is superposed to reduce the noise. The second harmonic signal superposed by Gaussian white noise and optical interference fringe is shown in Figure 2(c). The SNR is 19.1460 dB, and the peak SNR is 28.3 dB.

The IMFs components with different frequencies were obtained by CEEMDAN decomposition, as shown in Figure 3. The spectrum of the corresponding IMF component is shown in Figure 4. The Hurst index of each IMF component was calculated using the DFA principle, and the Hurst index value obtained was shown in Table I. According to Table I, the IMFs component with Hurst index value less than 0.5 was the first six order, that is, the first six order IMFs component was the noise dominant component.

The IMFs led by the information screened by DFA are reconstructed, and the reconstructed signal is denoised by wavelet soft threshold, and the final denoised signal is shown in Figure 5. Figure 5 shows that the 2f signal curve after denoising by CEEMDAN-DFA-WST is smooth. Compared with Figure 2(c), the denoising effect is more obvious. And good retention of useful information points.

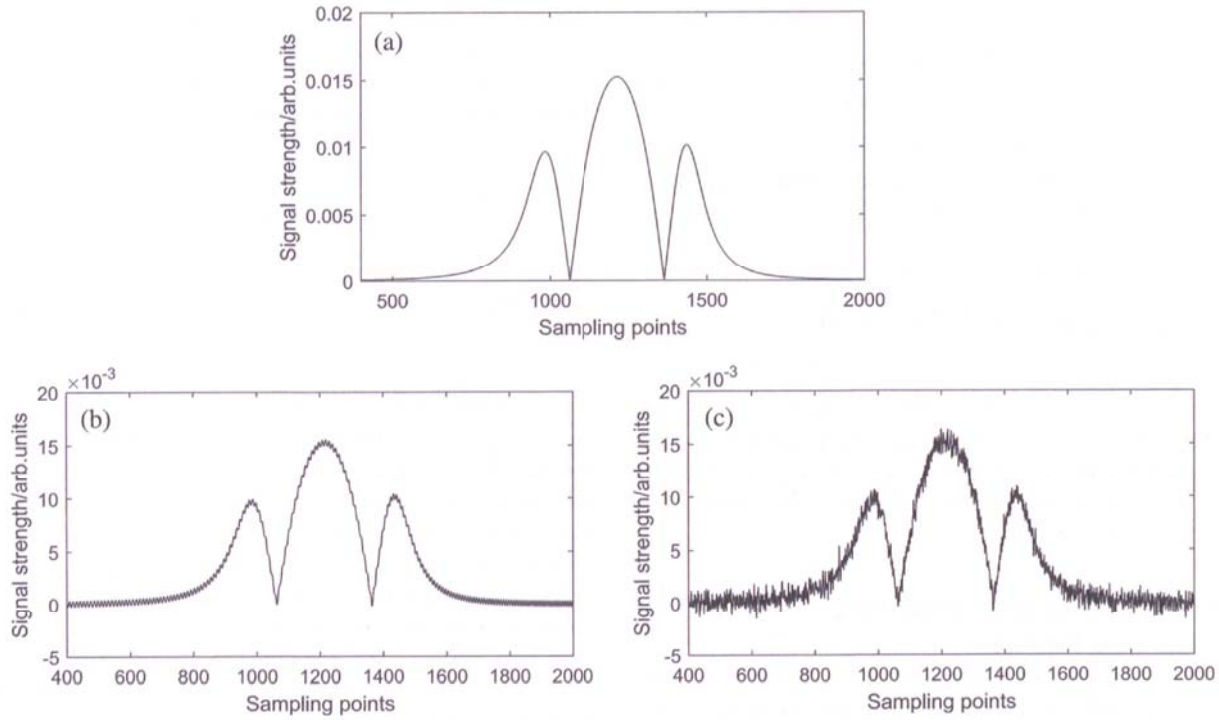

Fig. 2. Second harmonic signal; (a) Deal second harmonic signal; (b) Second harmonic signal superimposed by interference fringes (c) Second harmonic signal superimposed by white Gaussian noise and optical interference fringes.

3.3. CEEMDAN-DFA-WST Analysis of Noise Reduction Performance

To evaluate the denoising effect more accurately, mean absolute error (MAE), signal-to-noise ratio (SNR), peak signal-to-noise ratio (PSNR), and cross-correlation (CC) were used to evaluate the denoising effect. CEEMDAN-DFA-WST denoising algorithm is compared and analyzed with other denoising algorithms. Figure 6 shows the denoising results of different algorithms, and Table II shows the parameters obtained by comparing the denoising

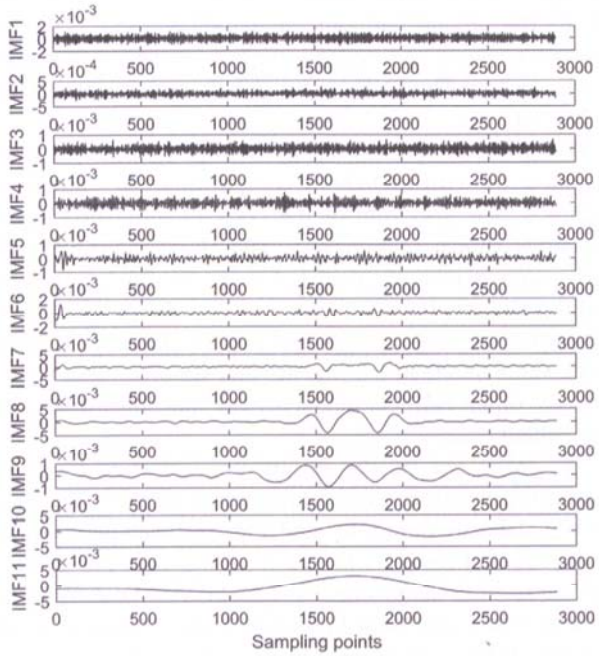

Fig. 3. IMFs component of noisy signal.

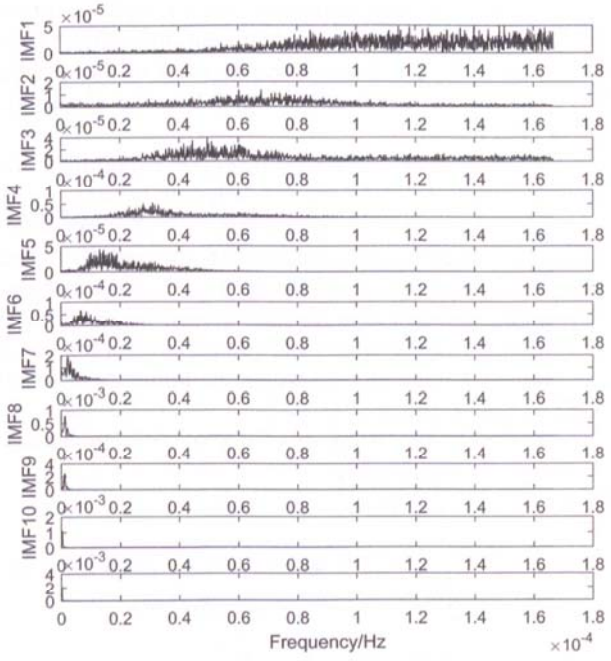

Fig. 4. Spectrum of IMF components.

Table I. Scale index of IMF components of the second harmonic signal.

IMF	1	2	3	4	5	6	7	8	9	10	11
α	0.1893	0.4072	0.1482	0.2179	0.3759	0.4012	0.7495	0.8524	0.8532	0.9999	1.0123

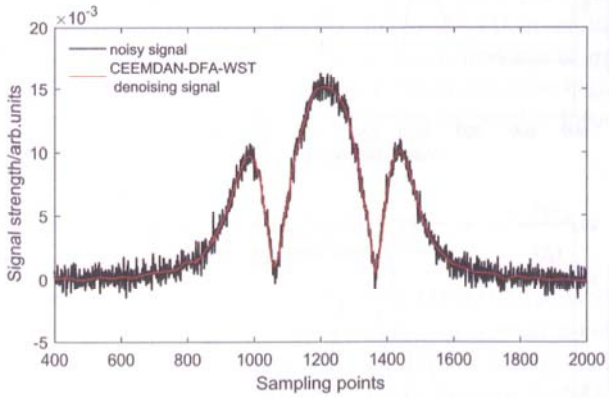

Fig. 5. Comparison of noise reduction effect of CEEEMDAN-DFA-WST.

effects of different algorithms. According to the data in Table II, the SNR of the second harmonic curve obtained by the CEEMDAN-DFA-WST denoising method is significantly increased compared with other denoising methods, from 19.1460 dB to 31.9750 dB, and the correlation is significantly enhanced to 99.9542%. Therefore, the second harmonic curve processed by the CEEMDAN-DFA-WST denoising method is closer to the original curve. This method has obvious advantages in noise reduction, and can well restore the peak position of the 2f signal, and retain the authenticity of the signal.

3.4. HHT-3D Spectrum is Used to Analyze the Noise Reduction Performance of Second Harmonic Signal

HHT-3D spectrum is a three-dimensional display of time-frequency characteristics of signals. Compared with Fourier transform analysis of signal frequency composition, the HHT-3D spectrum can analyze the change of signal frequency with time, which can better reflect the local characteristics of the signal [27]. Hibert-Huang includes EMD decomposition and Hilbert transformation [28]. Firstly, the EMD method was used to obtain the IMF components of each order, and then the instantaneous frequencies and corresponding amplitudes of each IMF component were obtained by Hilbert transform.

The corresponding HHT-3D spectra of the 2f signal with noise and the signal denoised by eight denoising algorithms are obtained respectively. From the HHT-3D spectra, the denoising effect of the denoising algorithm can be

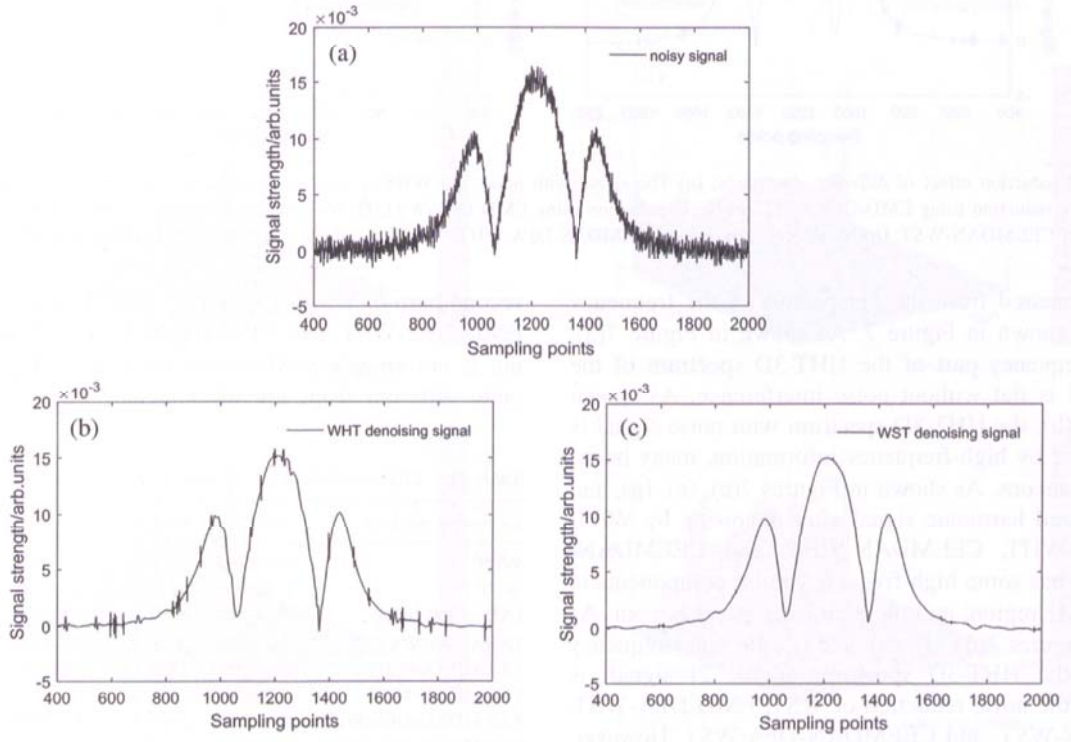

Fig. 6. Continued.

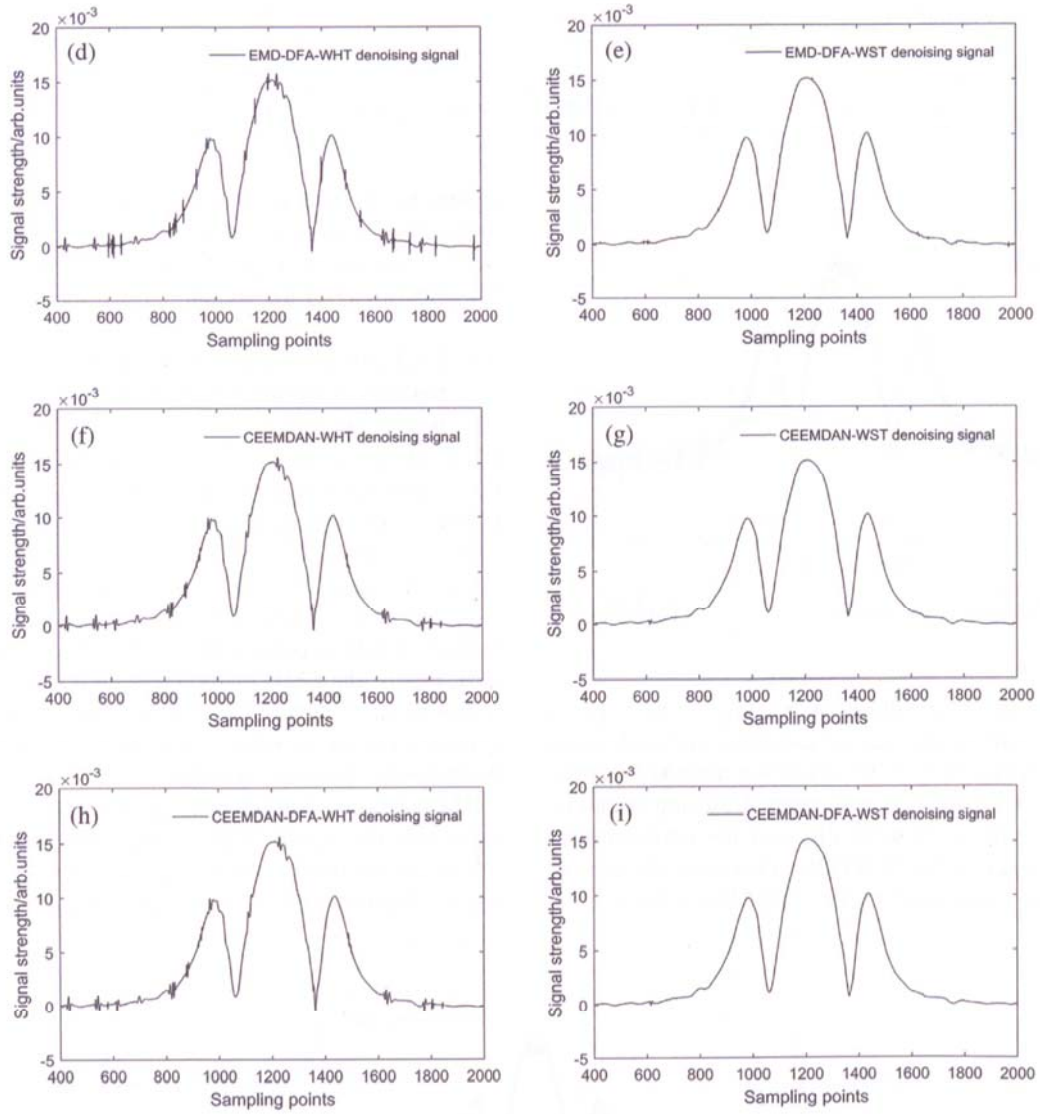

Fig. 6. Noise reduction effect of different algorithms; (a) The signal with noise; (b) WHT is used for noise reduction; (c) Noise reduction using WST; (d) Noise reduction using EMD-DFA-WHT; (e) Noise reduction using EMD-DFA-WST; (f) Noise reduction using CEEMDAN-WHT; (g) Noise reduction using CEEMDAN-WST; (h) Noise reduction using CEEMDAN-DFA-WHT; (i) Noise reduction using CEEMDAN-DFA-WST.

directly compared from the perspective of the frequency domain, as shown in Figure 7. As shown in Figure 7(a), the high-frequency part of the HHT-3D spectrum of the ideal signal is flat without noise interference. As shown in Figure 7(b), the HHT-3D spectrum with noise signal is characterized by high-frequency information, many burrs, and miscellaneous. As shown in Figures 7(c), (e), (g), and (i), the second harmonic signal after denoising by WHT, EMD-DFA-WHT, CEEMDAN-WHT, and CEEMDAN-DFA-WHT has some high-frequency noise components in the 0–400 Hz region, and the denoising effect is poor. As shown in Figures 7(d), (f), (h), and (j), the high-frequency region of the HHT-3D spectrum of the 2f signal. is clean after the noise reduction of WST, EMD-DFA-WST, CEEMDAN-WST, and CEEMDAN-DFA-WST. However, there is still some noise in the 0–200 Hz part of the second harmonic signal spectrum after denoising of WST, EMD-DFA-WST, and CEEMDAN-WST, and the denoising is not complete. Moreover, the HHT-3D spectrum is quite different from the ideal signal, which affects the

Table II. Effect evaluation of various denoising algorithms.

Denoising method	MAE/%	SNR/dB	PSNR/dB	CC/%
WHT	0.0160%	26.2841	35.5254	99.8302%
WST	0.0096%	31.7756	41.0169	99.9521%
EMD-DFA-WHT	0.0140%	27.9910	37.2323	99.8857%
EMD-DFA-WST	0.0096%	31.5982	40.8395	99.9504%
CEEMDAN-WHT	0.0125%	28.9161	38.1575	99.9075%
CEEMDAN-WST	0.0094%	31.8241	41.0655	99.9527%
CEEMDAN-DFA-WHT	0.0139%	28.1330	37.3743	99.8890%
CEEMDAN-DFA-WST	0.0094%	31.9750	41.2163	99.9542%

useful signal. However, the HHT-3D spectral features of CEEMDAN-DFA-WST are closer to the ideal signal as shown in Figure 7(a).

The analysis of the HHT-3D spectrum shows that the denoising effect of the algorithm combined with the wavelet soft threshold is better than that combined with the wavelet hard threshold. The denoising effect of the CEEMDAN-DFA-WST algorithm is superior to that of the second harmonic signal, which can better remove the high-frequency noise components and retain the useful information components of the low frequency.

4. RESULTS AND DISCUSSION

4.1. The Experimental Device

To verify the feasibility of the CEEMDAN-DFA-WST denoising algorithm, CO_2 gases with concentrations of 10%, 12%, 18%, and 20% were selected to extract their corresponding second harmonic signals. Figure 8 shows the structure of the experimental system. The system is composed of a signal generator, a DFB laser with a central wavelength of 1572.3 nm, a laser controller, a multi-reflector chamber with a 14.5 m optical path, a collimator, a photodetector, a lock-in amplifier, a data acquisition card, and a PC. The frequency of the sine wave modulation signal is set to 30 kHz, the voltage is set to 134 mV, the frequency of the sawtooth wave scanning signal is set to 10 Hz, and the tuning amplitude is set to 900 mV. Before each experiment, the gas absorption cell was repeatedly purged with high-purity N_2 to avoid interference from other gases in the air. The sine wave signal is generated by the signal generator and the sawtooth wave signal is superposed and input to the laser controller. The laser generated by the laser is absorbed by the gas chamber containing carbon dioxide, the absorbed signal is received by the photodetector, and the 2f signal is demodulated by the lock-in amplifier.

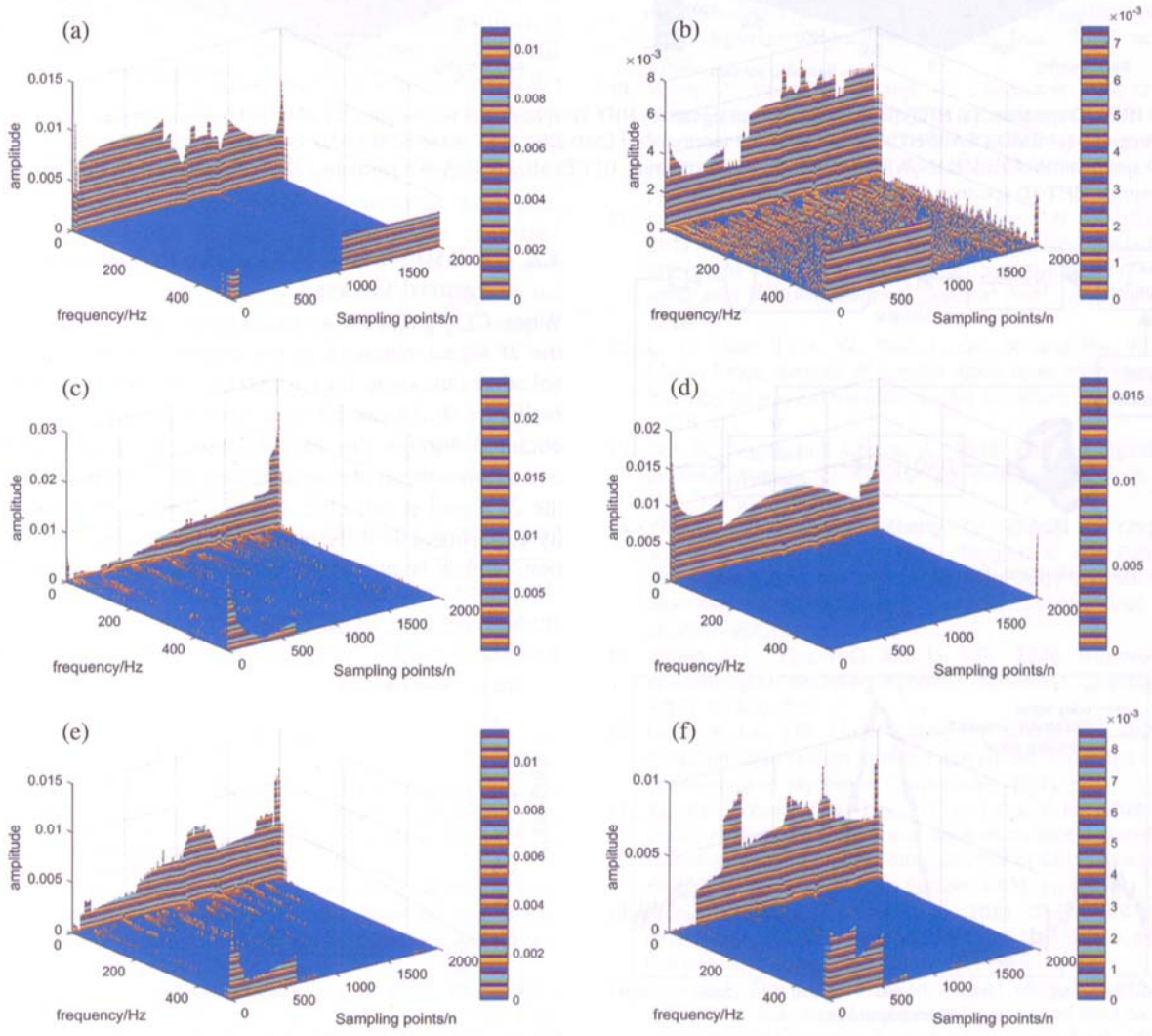

Fig. 7. Continued.

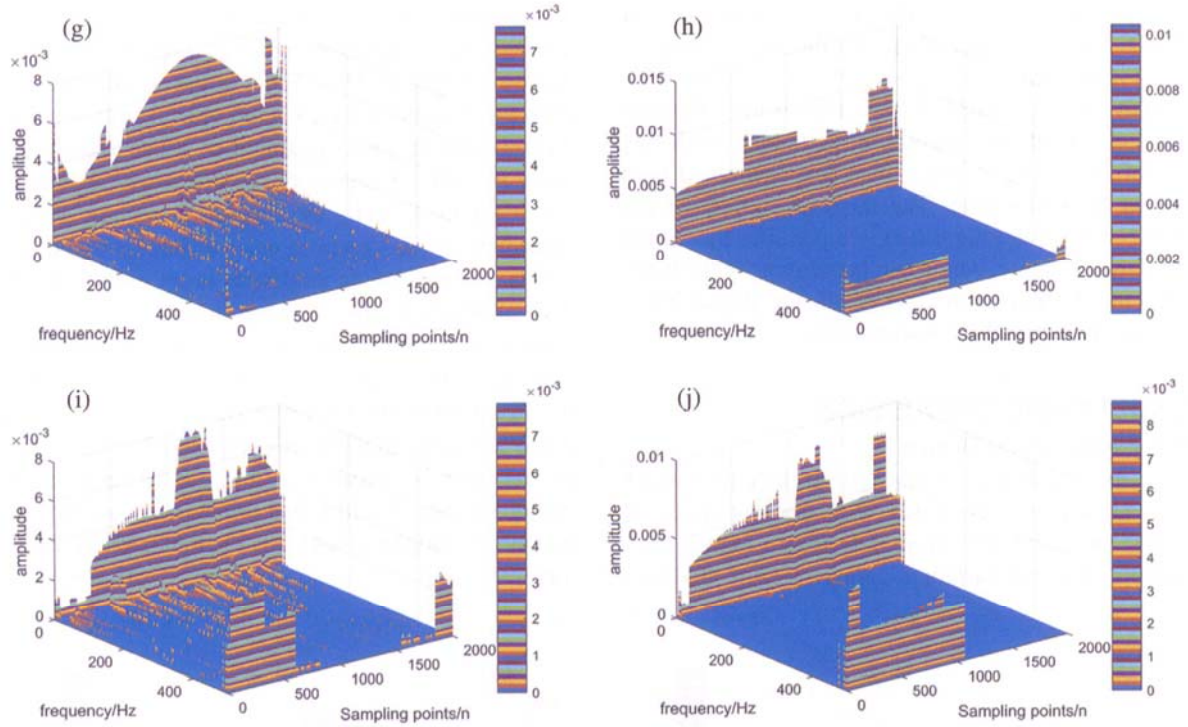

Fig. 7. HHT-3D spectrum; (a) HHT-3D spectrum of ideal signal; (b) HHT-3D spectrum of noise signal; (c) WHT HHT-3D spectrogram; (d) WST HHT-3D spectrogram; (e) EMD-DFA-WHT denoised HHT-3D spectrum; (f) EMD-DFA-WST denoised HHT-3D spectrum; (g) CEEMDAN-WHT denoised HHT-3D spectrum; (h) CEEMDAN-WST denoised HHT-3D spectrum; (i) CEEMDAN-DFA-WHT denoised HHT-3D spectrum; (j) CEEMDAN-DFA-WST denoised HHT-3D spectrum.

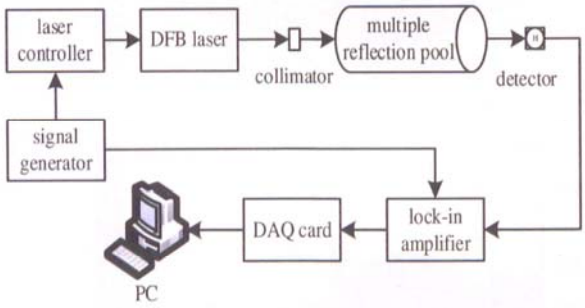

Fig. 8. System structure diagram.

4.2. CEEMDAN-DFA-WST Noise Reduction of Actual Measured Curves

When CO_2 gas with a concentration of 15% is injected, the 2f signal obtained in the experiment and the 2f signal after denoising by CEEMDAN-DFA-WST are shown in Figure 9. As can be seen from Figure 9, the 2f signal obtained through the demodulation of the lock amplifier is not smooth on the whole, and the amplitude point of the 2f signal is not clear enough. The 2f signal obtained by experiment is different from that obtained by simulation, which is not about center symmetry because it is

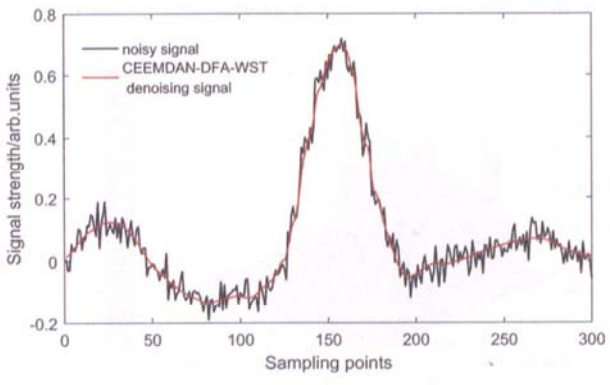

Fig. 9. Experimental data and denoised data of CEEMDAN-DFA-WST.

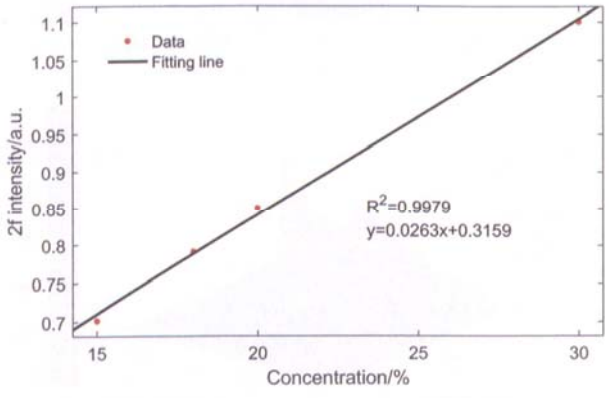

Fig. 10. Linear fitting of the relationship between the amplitude of the second harmonic and CO_2 concentration after denoising.

affected by the superposition of several harmonic components or residual amplitude modulation. The denoised 2f signal is smooth as a whole, and the denoising effect on useful information points is obvious. The linear fitting of the denoised 2f signal amplitude and CO_2 concentration is shown in Figure 10, the amplitude of the 2f signal is proportional to CO_2 concentration, and the linear correlation coefficient is 0.9979.

5. CONCLUSIONS

In this paper, a new CEEMDAN-DFA-WST denoising algorithm is proposed for the 2f signal of TDLAS technology. The CEEMDAN decomposition is used to decompose the 2f signal superposed by white Gaussian noise and optical fringes into intrinsic mode components of different frequencies. The detrended fluctuation analysis algorithm is introduced to screen the information-dominated eigenmode function, and the wavelet soft threshold denoising further improves the denoising accuracy and obtains a better denoising effect. By comparing with other noise reduction algorithms and analyzing the denoising effect, it can be seen that the SNR of this method is 31.9750 dB when processing the 2f signal. The correlation between the denoised 2f signal and the original 2f signal is stronger, and the correlation number is 99.9542%. The spectral characteristics of the signal denoised by various noise reduction algorithms of the HHT-3D spectrum were analyzed, and the effect of noise reduction was evaluated intuitively from the perspective of the frequency domain. The actual extraction of second harmonic signal noise reduction processing, the second harmonic signal amplitude linear fitting with gas concentration, R^2 is 0.9979, the noise reduction after the second harmonic signal of overall smooth, retain the useful information point, and achieved a good effect of noise suppression, in the combustion of gas concentration detection has a certain practical value.

Acknowledgments: This research was supported by the project of Jilin Province Science and Technology Development Program "Development of Intelligent Trace Inspection System Based on Polarization Imaging and multispectral Imaging" (Grant Numbers 20220203043SF).

References and Notes

1. Zhang, K., Zhu, W., Zhao, J., Lu, J. and Liu, T., **2019**. Study of vehicle exhaust detection based on TDLAS. *Optical Metrology and Inspection for Industrial Applications VI, 11189*, pp.286–294.
2. Pan, Y., Li, Y., Yan, C., Yuan, J. and Ren, Y., **2020**. Improvement of concentration inversion model based on second harmonic valley spacing in wavelength modulation spectroscopy. *IEEE Acceess, 8*(99), p.1.
3. Shao, J., Xiang, J., Axner, O. and Ying, C., **2016**. Wavelength-modulated tunable diode-laser absorption spectrometry for real-time monitoring of microbial growth. *Appl. Optics, 55*(9), pp.2339–2345.
4. Du, Z., Li, J., Cao, X., Gao, H. and Ma, Y., **2017**. High-sensitive carbon disulfide sensor using wavelength modulation spectroscopy in the mid-infrared fingerprint region. *Sens. Actuators, B, 247*, pp.384–391.
5. Zhu, C., Chang, J., Wang, P., Wei, W. and Zhang, S., **2015**. Continuously wavelength-tunable light source with constant-power output for elimination of residual amplitude modulation. *IEEE Sensors Journal, 15*(1), pp.316–321.
6. Yang, R., Dong, X., Bi, Y. and Lv, T., **2018**. A method of reducing background fluctuation in tunable diode laser absorption spectroscopy. *Optics Communication, 410*, pp.782–786.
7. Kireev, S.V., Kondrashov, A.A. and Shnyrev, S.L., **2019**. Application of the wiener filtering algorithm for processing the signal obtained by the tdlas method using the synchronous detection technique for the measurement problem of $13CO_2$ concentration in exhaled air. *Laser Phys. Lett., 16*(8), p.085701.
8. Xu, C., Wang, S., Chen, H., Wei, B. and Han, L., **2020**. Method for Eliminating Second Harmonic Distortion Based on Modulation Phase Difference in TDLAS Technology. *Sixth Symposium on Novel Photoelectronic Detection Technology and Application*, SPIE, Bellingham, Washington.
9. Cui, H.B., Yang, K., Zhang, L., Xiao-Song, W.U., Liu, Y., Wang, A., Li, H. and Ji, M., **2016**. Tunable diode laser absorption spectroscopy (TDLAS) detection signal denoising based on gabor transform. *Spectrosc. Spectral Anal., 36*(9), pp.2997–3002.
10. Wang, Z., Wang, Y., Zhang, R., Zhao, X.H., Liu, Q.J. and Cong-Rong, L.I., **2016**. A singular value decomposition method for tunable diode laser absorption spectroscopy system to remove systematic noises. *Spectrosc. Spectral Anal., 36*(10), pp.3369–3376.
11. Liu, Y.S., Jian-Jun, H.E., Zhu, G.F., Yang, C.H. and Gui, W.H., **2017**. A new method for second harmonic baseline correction and noise elimination on residual oxygen detection in packaged xilin bottle. *Spectrosc. Spectral Anal., 37*(8), pp.2598–2602.
12. Li, C., Guo, X., Ji, W., Wei, J., Qiu, X. and Ma, W., **2018**. Etalon fringe removal of tunable diode laser multi-pass spectroscopy by wavelet transforms. *Opt. Quantum Electron, 50*(7), p.275.
13. Cai, B., Su, B. and Collins, A., **2018**. Efficient digital signal process strategy for TDLAS gas detection. *J. Phys.: Conf. Ser., 1065*(25), p.252015.
14. Yi-Bing, L.U., Liu, W.Q., Zhang, Y.J., Zhang, K., Ying, H.E., You, K., Xiao-Yi, L., Liu, G.H., Tang, Q.X. and Fan, B.Q., **2019**. An adaptive hierarchical Savitzky-Golay spectral filtering algorithm and its application. *Spectrosc. Spectral Anal., 39*(9), pp.2657–2663.
15. Zheng, G.L., Zhu, H.Q. and Li, Y.G., **2020**. Improved LMS spectral signal denoising algorithm. *Spectrosc. Spectral Anal., 40*(2), pp.643–649.
16. Liang, Y., Liu, T.G., Liu, K., Jiang, J.F. and Li, Y.F., **2021**. Gas detection optimization method based on variationa-l modal decomposition algorithm. *China Laser, 48*(7), p.10.
17. Xu, F.H., Wang, Z.W., Liu, J.H. and Ou, W.M., **2020**. Application of combined EMD and wavelet threshold denoising in electrical imaging logging data. *Journal of China University of Petroleum, Natural Science Edition, 44*(3), pp.56–65.
18. Xiong, C.B., Wang, M. and Yu, L., **2021**. CEEMDAN-Wt combined noise reduction method for bri-dge GNSS-RTK deformation monitoring data. *Vib. Shock, 40*(9), pp.12–18.
19. Chang, J., Zhu, L., Li, H., Fan, X. and Yang, Z., **2018**. Noise reduction in lidar signal using correlation-based emd combined with soft thresholding and roughness penalty. *Optics Communication, 407*, pp.290–295.

20. Zhi, C., Feng, H., Xu, J., Xiang, Y. and Chao, M., **2017**. Comparative studies of wavelet threshold and complementary ensemble empirical mode decomposition in the denoising of differential column image motion lidar. *Optical Sensing and Imaging Technology and Applications, 10462*, pp.1258–1265.
21. Torres, M.E., Colominas, M.A., Schlotthauer, G. and Flandrin, P., **2011**. A Complete Ensemble Empirical Mode Decomposition with Adaptive Noise. *International Conference on Acoustics, Speech, and Signal Processing*, IEEE.
22. Li, Y., Xiao, C. and Jing, Y., **2019**. A hybrid energy feature extraction approach for ship-radiated noise based on CEEMDAN combined with energy difference and energy entropy. *Processes*, 7(2), p.69.
23. Cheng, Z., He, F., Zhang, S.L., Jing, X. and Hou, Z.H., **2017**. Combined wavelet-empirical mode decomposition method mod-ulated by trend term for atmospheric coherence length profile denoising. *J. Optics*, *37*(12), pp.15–26.
24. Li, R., Wang, J. and Chen, Y., **2018**. Effect of the signal filtering on detrended fluctuation analysis. *Phys. A*, *494*, pp.446–453.
25. Zhang, M., Lu, C. and Liu, C., **2019**. Improved double-threshold denoising method based on the wavelet transform. *OSA Continuum*, *2*(8), pp.2328–2342.
26. Chen, J., Li, X., Mohamed, M.a. and Tao, J., **2020**. An adaptive matrix pencil algorithm based-wavelet soft-threshold denoising for analysis of low frequency oscillation in power systems. *IEEE Access*, *8*, p.1.
27. Shiau, Y.H. and Wu, M.C., **2010**. Detecting characteristics of information masked by a laser-trigge-red microwave system via Hilbert-Huang transform. *Optics Communication*, *283*(9), pp.1909–1916.
28. Chen, L., Wang, C., Chen, J., Xiang, Z. and Hu, X., **2020**. Voice disorder identification by using Hilbert-Huang transform (HHT) and K nearest neighbor (KNN). *J. Voice*, *35*(6), p.932-e1.